2019 Rock Dynamics Summit– Aydan et al. (eds)
© 2019 Taylor & Francis Group, London, ISBN 978-0-367-34783-3

The behaviour of Oya tuff pillars under static and shock loading

T.K.M. Dintwe
Kyushu University, Fukuoka, Japan

T. Seiki
Utsunomiya University, Utsunomiya, Japan

Ö. Aydan & N. Tokashiki
University of the Ryukyus, Okinawa, Japan

ABSTRACT: Earthquakes have caused some damage to abandoned quarries in Oya region, Japan and the behaviour of pillars of Oya tuff quarries is therefore of paramount importance for the region. This study reports investigation results of Oya tuff pillars under static and dynamic conditions. Also, the backfilling of underground quarries is considered as a countermeasure of collapse in the long term and during earthquakes. For this purpose, an experimental laboratory program was initiated to investigate the static and dynamic response of Oya tuff pillars. The shock tests demonstrate that the overall stiffness of samples subjected to shock loading is higher than that of samples under static loading. With respect to backfilling, the results show that, the overall stiffness of backfilled samples is higher than that of unfilled and in some cases, the yielding strength of backfilled samples displays strain hardening behaviour, while unfilled samples show strain softening behaviour. Different degrees of backfilling, indicate that partial backfilling is not effective to prevent ground settlement.

1 INTRODUCTION

Underground structures have been known to be seismically insulated or rather could sustain seismic loads with little damage. However, over recent years the investigations regarding seismic response reveal that underground spaces such tunnels and underground shallow mines could experience significant damages (Wang, et al., 2001; Genis & Aydan, 2008; Aydan, et al., 2010). Unlike in deep mines, where stress-induced failures can occur in a violent manner invoking seismic events, in shallow mines, the type of dynamic loading that could pose a threat to shallow mines is the occurrence of the earthquake. In Japan, there are several cases in which underground spaces have been damaged by the often occurrence of earthquakes. After the 2011 Great Earthquake of East Japan with the magnitude of 9 (Aydan, 2014) embarked on the expedition visiting the affected areas focusing on the various damaged geo-engineering structures, and with special interest to abandoned underground mines and quarries. Aydan, (2014) documented and summarized almost all the accessible damaged underground areas. The records show that the earthquake caused sinkholes in several locations Iwaki in the Fukushima Prefecture, eleven locations in Kurihara, seven locations in Osaki, eleven locations in Higashi Matsushima, three locations in Kurogawa in the Miyagi Prefecture (Aydan & Tano, 2012a). It was later mentioned by the Ministry of Economy, Trade and Industry (METI) that the actual number of the sinkholes is more than 316. Still from the list, it is interesting to note that one of the collapsed mines is the semi-underground mine located in Oya town in Tochigi prefecture and this collapse is not far from the area of the underground room and pillar quarry that is understudy. There is still an apprehension of similar cases reoccurring due to the influence of dynamic loading. A recent study by Seiki, et al., 2016 on seismic responses of long-wall type quarry 2km away from the current study area, has shown that increase in wave velocities results in high strain levels on the roofs walls. With all these past studies revealing the problems associated with dynamic loading in various underground spaces, a dynamic response investigation of pillars serves to be necessary and an essential study that could give fundamental understandings for underground mine stability.

Laboratory tests are a good start to investigate rock material response under dynamic loading. However, dynamic tests were often viewed as challenging due the loading rate needed and data recording. Specialized equipment is often a requirement to be able to carry out such test. Most studies on dynamic properties of material were demonstrated using the split Hopkinson pressure bar (SHPB) (Niu, et al., 2015). With SHPB the dynamic properties of the solid material could be captured and enables to estimate the work done on the material. Over the years the dynamic response of rock material under dynamic loading has been studied (Okubo, et al., 1990; Hashiba, et al., 2006; Chen, et al., 2005; Li, et al., 2008; Aydan, et al., 2010). Specifically, for shock or impact loading tests, not sufficient studies have been done, however it is appropriate to mention the work by Li, et al., 2007; Niu, et al., 2015; Aziznejad, et al., 2018. The three independent studies highlight the importance of the shock test in rock engineering. To simulate ground motions, a shaking table test could be used on room and pillar models and assess the response as demonstrated by Aydan, et al., 2010.

The subsidence incidents that took place in Japan dictate that regional support is the ultimate solution and the probable support for the abandoned mine would be backfilling. Backfilling in dynamic states hinder stopes and pillar to vibrate in critical resonant frequencies (Goldbarch, 1991), hence reducing risk of collapse. The other component of interest is the pillar size, thus the width to height (*w/h*) ratio. The optimum pillar size is desirable to have high production (high extraction ratios). High extraction ratios results in slender pillars or few pillars in the layout. The determination of the pillar size does not consider production only, but also the stability of the pillar, which plays important role in the safety success of the mine. That is very slender pillars could cause stability problems and high *w/h* ratios would reduce production.

Therefore, this study attempts to understand the effect of shock loading in rocks particularly Oya tuff through a series of tests in static and shock loading and observing the rock response. Finally, backfilling is introduced in the experiment and investigated as countermeasure for pillar failure.

2 METHODOLOGY

2.1 *Sample preparation*

There are specimen dimension standards for performing Uniaxial Compression strength (UCS) tests, typical standard size in width to height ratio is 0.5 with a 100mm height, and this was adopted for the experimental tests. However, in this study the test is pillar oriented laboratory testing, so the pillars are to be in bounded between two cylindrical blocks of (Ryukyu lime stone) that act as the roof and floor of quarry. It is ideal to use sample rock type for roof and floor as it is the case in the actual field. In some instances, the top blocks may also fail when the rock type is same as the pillar during the test or in the field where pillar are observed to have punched into the foundations (Ryder & Jager, 2002). Nevertheless, the pillar behaviour could be assessed despite the rock type of top and bottom blocks. Samples with square cross section were preferred since the pillars in the quarry are mostly square pillars. The samples were saw cut out from large blocks prepared by the mining company to the specified dimensions with *w/h* ratios, 0.3, 0.5 and 1 respectively.

2.2 *Experimental setup and instrumentation*

A cylindrical acrylic vessel with internal diameter of 100 mm, a height of 250 mm and 10 mm thickness was used for investigating the support effect of sand granular backfilling on Oya tuff pillar samples. The standard size of pillar sample was 48-51mm in width and 98 to 100 mm in height. The Ryukyu limestone block have dimensions of 100 mm height and 98 mm diameter, see (Fig. 1) for the conceptual model. The experiments were performed under servo controlled machine with capacity of 2000 kN and loading rates ranging between 0.7 to 1.0 MPa/s. The experimental setup allows for multi-parameter monitoring. The load acting on the pillars was continuously monitored together with the displacement, acceleration, and acoustic emission (AE). Before and after each compression test p and s wave velocities were measured.

In dynamic test, shock load was applied on sample to obtain the shock strength of the rock still using the conventional compression test machine. The machine is not actually designed for dynamic loading; however, the loading was done instantly such that it could represent shock loading. With the limitations of the

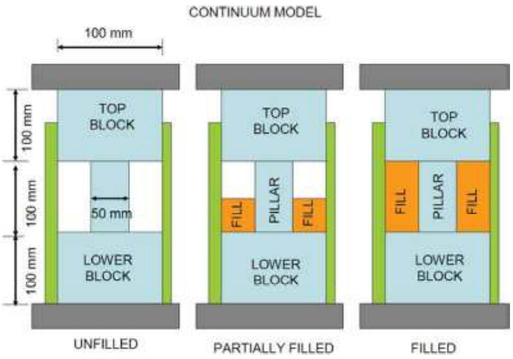

Figure 1. Conceptual setup of the pillar-oriented test

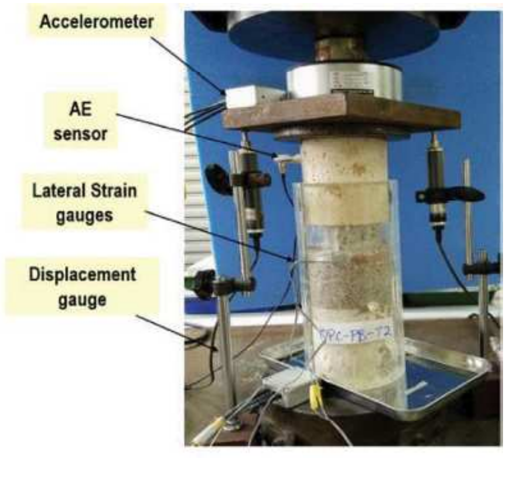

Figure 2. Experimental setup of the pillar-oriented test

machine in mind some of the results in this method are to be compared with those of a specialized machine designed for shock loading in future publications. Even though the earthquake loading is complex cyclic loading and could result in different damage mechanism of the rock, the shock test gives a somehow representation of the vertical component of the earthquake wave. The loading rate estimation is from load-time graph and could be calculated as follows:

$$r = \frac{\Delta l}{\Delta t} \equiv \frac{l_p}{t_p} \tag{1}$$

where l_p is the maximum load (kN) or the peak load and t_p is the time (s) taken from the start of the test until reaching the peak load.

For backfilling, sand is used as the backfill material and similar procedure as the static and dynamic test is used with the difference being that the sample is surrounded by sand. Two types of backfill test were carried out as previously mentioned; the first sample was partially filled to about 70% of the pillar height and load applied until failure and still continuously monitoring. The second part of the backfill experiment is to entirely fill the pillar sample with granular sand material. The tangential strain of the backfill material used in the compression test was monitored on the outer walls of the acrylic cell.

3 EXPERIMENTAL RESULTS

3.1 *Static tests (Uniaxial)*

Figure 3 shows the load-time graph of the pillar samples. The graph shows all the multi parameters measures recorded during the static test experiment, except the acceleration. The relationship among the parameters surely is commensurate. The increase and decrease in the load is clearly detected by the AE. The load was constantly increasing until the rock failure, where a sudden vertical increase is noticed. The trend on the load and displacement is reflected in the cumulative AE, and the time of events actually coincides.

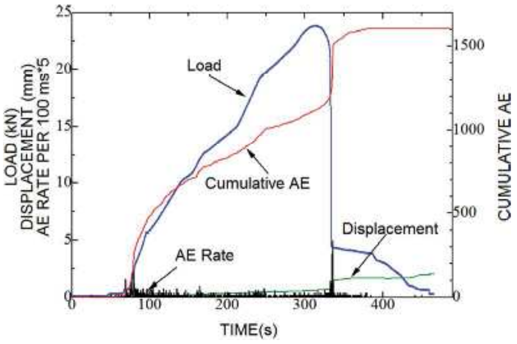

Figure 3. Load displacement curve and AE counts for static test

Figure 4 depicts the typical stress-strain curve of Oya pillar sample obtained from the experiment. The young modulus is estimated from this curve, and the average strength (UCS) of Oya tuff is 8.6MPa. The three phases of the stress strain curve are outlined, yield, peak and residual. Table 1 summarizes physical and mechanical parameters of the intact Oya tuff.

3.2 *Shock test (Uniaxial)*

The loading rate of the shock test is 187kN/s (75 MPa/s). Similar to the static experiment, the shock test failure was detected by AE and the corresponding displacement was observed see (Fig. 5). Upon assessment of the loading history, all the micro loads acting on the sample while attempting to apply the shock load are recorded. This type of testing will require several

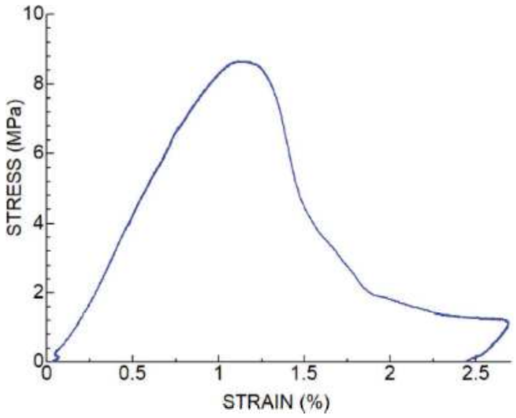

Figure 4. Stress-strain curve for static test

Table 1. Physico-mechanical properties of Oya Tuff (static)

Density	Shear modulus (GPa)	Bulk modulus (GPa)	Compresive strength (MPa)	Cohesion (MPa)	Tensile strength (MPa)
2400	0.91	1.28	8.6	2.1	1.08

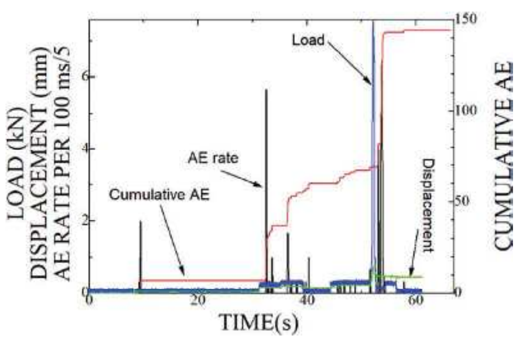

Figure 5. Load-displacement curve and AE counts responses for shock test

samples to get the test right and personnel experience is vital. The records before about 50 seconds are missed shock loadings; this highlights the difficulty of using the conventional machine for dynamic shock testing. Despite the limitations, attempts were made and successful tests were recorded. Figure 6 shows the stress-strain curve of the shock test. In the figure, it is clear that the shock curve peak strength is higher than that of the samples tested under static loading. It is also observed that stiffness of the samples is higher in shock loading. The acceleration has varied response signatures according to position of the accelerometer and the loading rate. Figure 7(a-b) show the acceleration history of the static test and shock tests. The acceleration results presents only the vertical component of the system. This is simply due to the fact that the loading is applied in the vertical direction. Generally, the accelerations from the top platen positions are much higher than the bottom platen where noise is usually recorded, hence only the top platen acceleration presented, and obviously the shock tests result in higher acceleration peaks than static tests. Having much higher peaks in the top platen accelerometers is a result of the mobile part gaining more acceleration after the sample failure than the stationary bottom part (Aydan, 2004).

3.3 *Effects of w/h ratio*

The aspect ratio is well-known to have effects on the pillar strength, and substantial research has covered this area. Past experimental work on Oya tuff has been done to estimate static mechanical properties regarding the aspect ratio. However, dynamic properties of various aspect ratios are still yet to be determined. The procedure for both static and shock UCS tests was repeated for additional aspect ratios namely, 0.3 and 1. Figures 8 and 9 show the aspect ratio results of the static and shock tests respectively. The results are startling; it is well known that the pillar strength increase with increasing *w/h* ratio, however the results are showing the opposite of this fact. The strength of the pillar shows to be increasing with decrease in *w/h* ratio. This relationship trend is observed in both the static and shock tests results.

3.4 *Backfilling*

3.4.1 *Static test*

As stated before that the degree of backfilling is of interest, Figure 10 presents load-displacement vs time together with other parameters of the partially

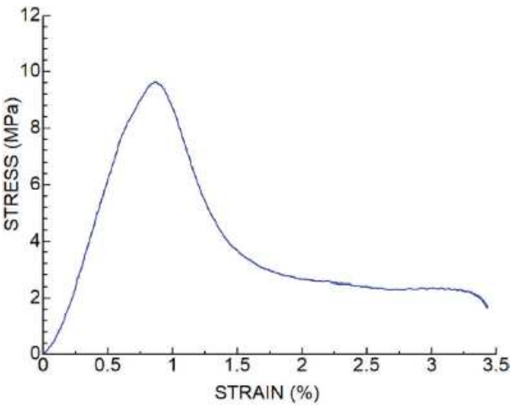

Figure 6. Stress-strain curve for shock test

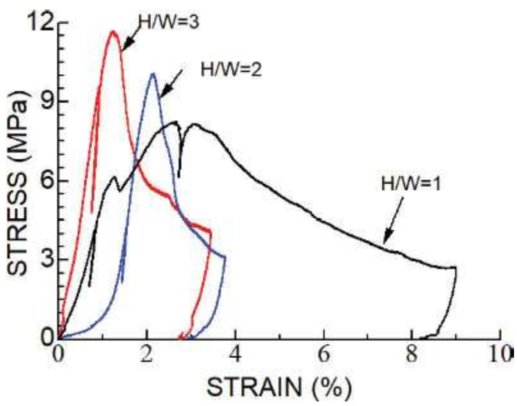

Figure 8. Stress-strain curve for various pillar geometry under static loading

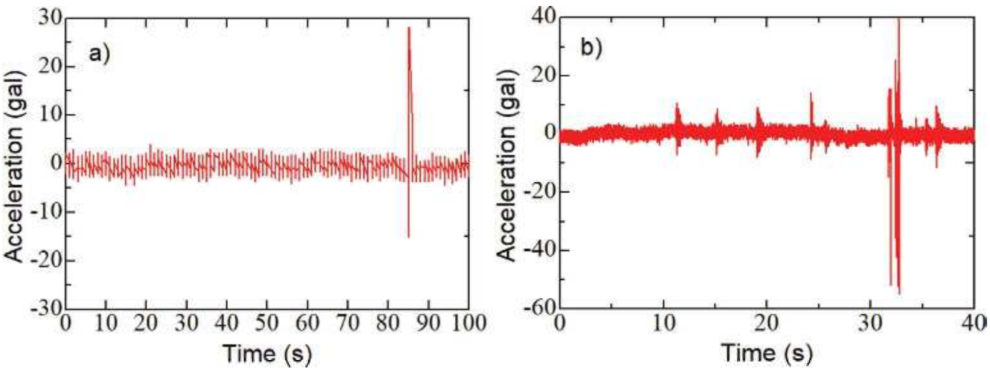

Figure 7. Acceleration response of samples a) top platen (static) b) top platen (shock)

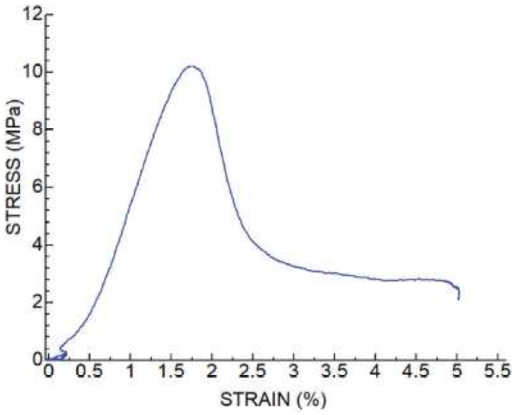

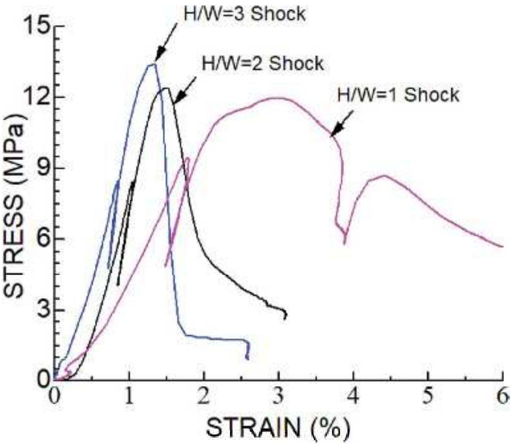

Figure 9. Stress-strain curve for various pillar geometry under shock loading

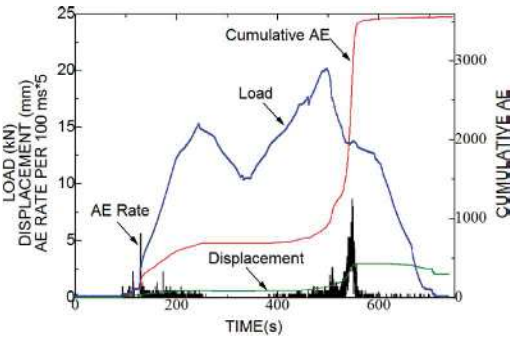

Figure 10. Load-displacement curve, AE counts for partially filled sample

filled pillar sample (PSB). The load curve indicates that the sample had failed under loading and then loaded again (cyclic loading). The pillar samples load bearing capacity has increased after failure and this surely due to the confinement offered by the sand backfill. Just like in the non-backfill sample (NSB) test, the AE rate increases as the load increases and decrease when the samples undergo unloading. Furthermore, permanent straining is observed after loading and unloading cycle even though it is just one cycle. The full backfill pillar sample (FSB) results are shown in Figure 11; the sample was loaded in three cycles. It is interesting to note that the drop in the loading does not mean that the sample had failed, rather the loading was terminated as the strength was progressively increasing in strain hardening behaviour and could cause bursting of the acrylic cell. Also the displacement shows an increase in the first 200 secs, thereafter it remains relatively constant until experiment termination. Like the previous test, the AE rate is directly proportional to the load, whereas the cumulative AE still shows permanent straining and in this case it was sharply increasing and Kaiser-effect (K.E) is noted from the measured responses. The results are in correspondence with those observed by Aydan (2013). The comparison of the three conditions of the continuum pillar sample; NSB, PSB, FSB are all compared in Figure 12. It is clearly seen that the brittle failure manner is pronounced in the NSB sample, while the PSB sample undergoes the strain softening failure manner,

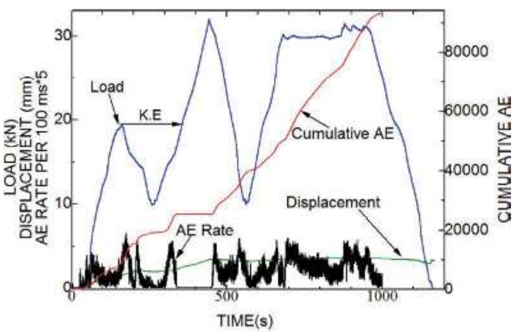

Figure 11. Load-displacement curve, AE counts response for full backfill sample

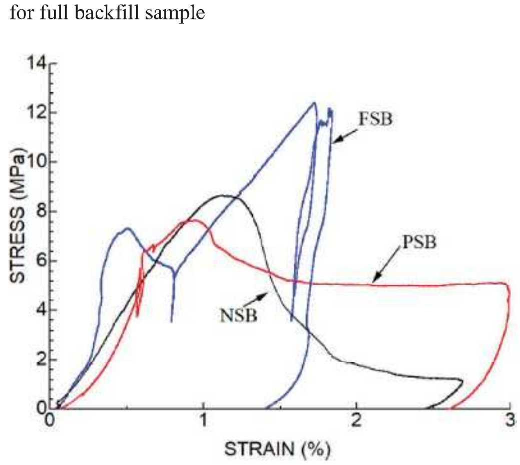

Figure 12. Stress-strain curve for various backfilling degrees under static loading

and it shows a much higher residual strength than the NSB sample. In the case of the FSB, the bearing capacity increased to about 1.5 times that of the unfilled pillar sample. The backfill cases reveal that after yielding or even before that, the backfill material that takes over the load with the rock, and sustain further cyclic loading and display strain-hardening. Thus, the backfill material alters the overall stress-strain response (Aydan, et al., 2013).

3.4.2 *Shock test*

The three cases of NSB, PSB and FSB compression test are repeated under shock loading. The results are presented in the stress-strain curves in Figure 13. No-backfill curve display low stiffness as compared to other graphs. Stiffness show to be increasing with the addition of backfill and highest stiffness is achieved with full backfilling. The peak strength of the PSB appear to be the highest in this case, however, the FSB samples did not show clear fracturing as the PSB samples.

3.5 *Failure characteristics of samples*

The pillar samples were then assessed after the experiment and have a closer look at the failure planes. Figure 14 (a-c) shows the photos of the continuum pillar samples after the UCS test, the NSB sample shows well-defined tensional crack (mode I), and the PSB sample has failed more like under triaxial conditions due to confinement provided by the backfill. Clear shear fractures are observed on the partially filled sample forming under the maximum principal stress $\boldsymbol{\sigma}_1$. The movement on the shear fractures is parallel to the fracture surface (mode II & III). Since the stress state in the PSB acts as in triaxial ($\boldsymbol{\sigma}_1 > \boldsymbol{\sigma}_2 \geq \boldsymbol{\sigma}_3$), the fracture planes form a conjugate pair (conjugate shear fractures). Under a true triaxial test with well controlled conditions or confinement, the angle between the conjugate fractures may be bisected by the maximum principal stress $\boldsymbol{\sigma}_1$. The FSB sample is still intact, no visible fractures with naked eye, and this require more magnified assessment of the sample by using high resolution camera, and minute size extensional fractures were observed on the surface of the pillar sample.

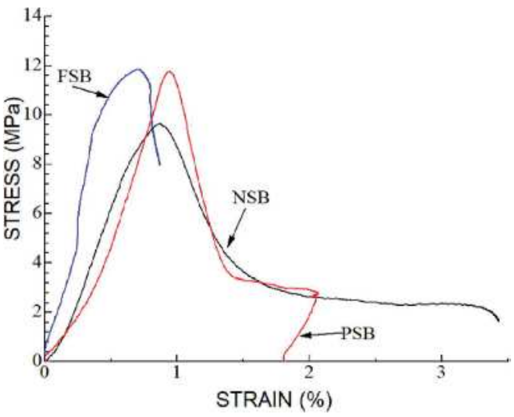

Figure 13. Stress-strain curve for various pillar geometry under shock loading

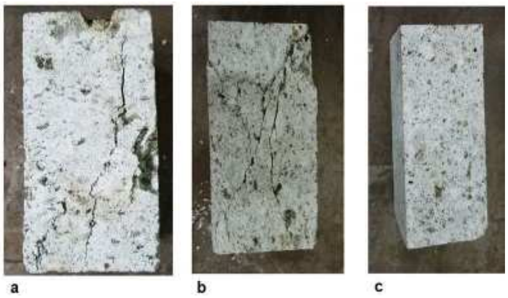

Figure 14. Failed samples under different backfill degrees a) unfilled b) partial-backfill c) full-backfill

4 CONCLUSION

An experimental study investigating the behaviour of Oya tuff pillars under static and shock loading was carried out. The shock loading has shown to be possible with conventional compression machine despite its limitations. The static and shock loading test results have been compared and analysed. It was found out that the overall stiffness of the pillar sample subjected to shock loading is higher than those of the samples under static loading. The strength of samples tends to increase with the decrease in *w/h* ratio which is normally not the case, rather the strength has to be increasing with the ratio. The authors are very aware that the aspect ratio results are somewhat different from the previous studies. Therefore, further work is to be conducted to understand what could have caused the outcome.

The experiments demonstrate that the stiffness of backfilled samples is higher than those of unfilled samples. Backfilling increases the bearing capacity, and results in peak and residual strength of backfilled samples being much higher than the unfilled samples. In some cases, backfilled samples display strain hardening behaviour while the unfilled display strain softening behaviour. Different degrees of backfilling indicate that partial backfilling is not effective to prevent settlement as compared to full backfill.

REFERENCES

Aydan, Ö., 2004. An Experimental Study on Dynamic Responses of Geo-Materials during Fructuring. *Journal of The School of Marine Science and Technology*, 1(2), pp. 1–7.

Aydan, Ö., 2014. Crustal stress changes and characteristics of damageto geo-engineering structures induced by the Great East Japan Earthquake of 2011. *Bull Eng Geol Environ (2015) 74:1057–1070*, p. 1064.

Aydan, Ö. et al., 2010. Response and stability of underground structures in rock mass during earthquakes. *Rock Mech Rock Eng*, pp. 857–875.

Aydan, Ö. & Tano, H., 2012a. The damage to abandoned mines and quarries by the Great East Japan Earthquake on March 11, 2011. Tokyo, s.n., pp. 981–992.

Aydan, Ö., Tokashiki, N. & Tano, H., 2013. An experimental study on te supporting effect of backfilling on an abandoned room and pillar mines, quarries and karstic caves, and its in-situ verification. s.l., American Rock Mechanics Association.

Aziznejad, S., Esmaieli, K., Hadjigeorgiou, J. & Labrie, D., 2018. Responces of jointed rock masses subjected to impact loading. *Journal of Rock Mechanics and Geotechnical Engineering*, pp. 624–634.

Chen, F., MA, C.-d. & XU, J.-c., 2005. Dynamic responce and failure beahaviour of rock under static-dynamic loading. *J. Cent. South Uni. Technol*, 12(3), pp. 354–358.

Genis, M. & Aydan, Ö., 2008. *Assessment of Dynamic Response and Stability of an Abandoned Room and Pillar underground Lignite Mine*. Goa, s.n., pp. 3899–3906.

Goldbarch, O. D., 1991. *Ground motion studies in a backfilled stope at West Driefontein*, Johannesburg: s.n.

Hashiba, K., Okubo, S. & Fukui, K., 2006. A new testing method for investigating the loading rate dependency of peak strength and residual rock strength. *International Journal of Rock Mechanics & Mining Sciences*, pp. 894–904.

Li, X. et al., 2007. Innovative tesiting technique of rock subjected to coupled static and dynamic loads. *International Journal of Rock Mechanics & Mining Sciences*, pp. 739–748.

Li, X. et al., 2008. Innovative testing technique of rock subjected to coupled static and dynamic loads. *International Journal of Rock Mechanics & Mining Sciences*, pp. 739–748.

Niu, Y. et al., 2015. Experimental study on Shock Mechanical Properties of Red Sandstone under Preloaded 3D Static Stress. *Journal of Engineering Science and Technology Review*, pp. 205–2011.

Okubo, S., Nishimatsu, Y. & He, C., 1990. Technical Note: Loading Rate Dependence of Class II Rock Behaviour in Uniaxial and Triaxial Compression Tests-An Application of a Proposed New Control Method. *Int.J.Rock Mech Min.Sci.& Geomech.Abstr.*, 27(6).

Ryder, J. A. & Jager, A. J., 2002. Mechanical Properties of Rock. In: *Rock Mechanics For Tabular Hard Rock Mines*. Johannesburg: The Safety in Mines Research Advisory Committe(SIMRAC), pp. 1–60.

Seiki, T. et al., 2016. Seismic response of numerical analysis and field measurement in Oya tuff qurry. *Eurock*, p. 8p.

Wang, W. L. et al., 2001. Assessment of damage in mountain tunnels due to the Taiwan Chi-Chi Earthquake. *Tunnelling and Underground Space Technology*, Volume 16, pp. 133–150